

Phenanthrenes from *Juncus inflexus* with Antimicrobial Activity against Methicillin-Resistant *Staphylococcus aureus*

Barbara Tóth,[†] Erika Liktör-Busa,[†] Norbert Kúsz,[†] Ádám Szappanos,[‡] Attila Mándi,[‡] Tibor Kurtán,[‡] Edit Urbán,[§] Judit Hohmann,^{†,⊥} Fang-Rong Chang,^{*,||,#,¶} and Andrea Vasas^{*,†}

[†]Department of Pharmacognosy and [⊥]Interdisciplinary Centre of Natural Products, University of Szeged, 6720 Szeged, Hungary

[‡]Department of Organic Chemistry, University of Debrecen, 4032 Debrecen, Hungary

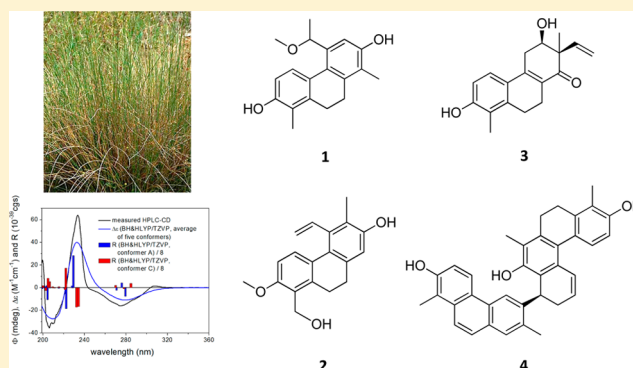
[§]Institute of Clinical Microbiology, University of Szeged, 6725 Szeged, Hungary

^{||}Graduate Institute of Natural Products, College of Pharmacy, and [¶]Research Center for Environmental Medicine, Kaohsiung Medical University, 807 Kaohsiung, Taiwan

[¶]Department of Marine Biotechnology and Resources, National Sun Yat-sen University, 804 Kaohsiung, Taiwan

Supporting Information

ABSTRACT: The present study has focused on an investigation of the antibacterial effects of *Juncus inflexus* and the isolation and identification of its active compounds. Eleven phenanthrenes were isolated from a methanolic extract of the roots. Four compounds (jinflexins A–D, 1–4) are new natural products, while seven phenanthrenes [juncuenins A (5), B (6), and D (8), juncusol (7), dehydrojuncuenins A (9) and B (11), and dehydrojuncusol (10)] were isolated for the first time from the plant. Jinflexin D (4) is a dimer with an unprecedented heptacyclic ring system. The absolute configurations of the new compounds were determined by TDDFT-ECD calculations, and their enantiomeric purity was checked by chiral HPLC analysis. Extracts of different polarity (*n*-hexane, dichloromethane, and ethyl acetate) were evaluated for their antimicrobial effects against methicillin-resistant *Staphylococcus aureus*, extended-spectrum β -lactamase (ESBL)-producing *Citrobacter freundii*, *Escherichia coli*, *Enterobacter cloacae*, *Klebsiella pneumoniae*, multiresistant *Acinetobacter baumannii*, and *Pseudomonas aeruginosa*. The MIC values of the isolated compounds were determined by a microdilution method. Jinflexin B (2), juncusol (7), juncuenin D (8), and dehydrojuncuenin B (11) showed significant activity (MIC value range 12.5–100 $\mu\text{g}/\text{mL}$) against MRSA strains.



Microbial infections and diseases are one of the leading causes of deaths worldwide after cardiovascular diseases. *Staphylococcus aureus* is a major pathogen since it possesses extreme genetic plasticity. Hence, owing to bacterial evolution and drug abuse, the resistance of *S. aureus* has increased dramatically. Methicillin was introduced in therapy in 1959 in order to treat penicillinase-producing *S. aureus* infections,¹ but this bacterium rapidly acquired resistance. The first methicillin-resistant *S. aureus* (MRSA) strains were identified in 1961 in the United Kingdom.² MRSA is becoming resistant to the most recently developed antibiotics, with the options for the successful treatment of MRSA being very limited.³ Moreover, MRSA variants pose a real threat to become untreatable multidrug-resistant bacteria,⁴ so there is an urgent need for novel anti-MRSA agents with new modes of action.

During their evolution, plants developed different defense mechanisms and systems in order to protect themselves against abiotic (e.g., UV radiation)⁵ and biotic stresses (e.g., microorganisms).⁶ Natural products from plants could therefore be

interesting alternatives in antibiotic therapy, because plants produce these compounds in part in order to defend themselves from microbes.

The family Juncaceae comprises approximately 500 species worldwide, and these are distributed into seven genera.^{7,8} The largest genera are *Juncus* ($n = 347$) and *Luzula* ($n = 140$). There are 15 *Juncus* and six *Luzula* species native to Hungary. Most of the *Juncus* species grow exclusively in wetland habitats. In traditional oriental medicine, the medulla of *J. effusus* has been used for the treatment of colds, insomnia, and anxiety.^{9,10} An infusion of *J. acutus* fruits mixed with grains was applied for the treatment of cold and fever.¹¹

The most characteristic compounds identified in the species of the family Juncaceae are phenanthrenes and 9,10-dihydrophenanthrenes. These compounds are derived from a specific biosynthetic pathway, presumably formed by oxidative

Received: June 24, 2016

proton as a singlet (δ_{H} 6.86), three methyls, two methylenes, one sp^3 methine, and signals of protons belonging to one methoxy and two hydroxy groups. In the JMOD (*J*-modulated spin-echo experiment) spectrum, the presence of 19 carbon signals was detected (Table 1). In the ^1H NMR spectrum, two methylene signals at δ_{H} 2.32 and 2.75 ($2 \times 2\text{H}$) indicated this compound to be a 9,10-dihydrophenanthrene derivative. In the ^1H - ^1H -COSY spectrum, correlations were observed between the H-9 and H-10 methylenes, δ_{H} 6.70 and 6.84 d (H-3/H-4), and δ_{H} 4.69 and 1.47 d (3H) (H-12/H-13). The methyl doublet at δ_{H} 1.47 and a methine proton at δ_{H} 4.69 provided evidence for the presence of an isolated CH_3CH structural unit (C-12, C-13) in the molecule. According to the ^1H and ^{13}C NMR signals at δ_{H} 2.85 and δ_{C} 55.0, a methoxy group could be identified, which was connected to C-12 as confirmed by an HMBC correlation between OCH_3 (δ_{H} 2.85) and C-12 (δ_{C} 74.5) (Table 1). Moreover, on the basis of HMBC correlations between C-5/13-Me, C-6/H-12, and C-5a/H-12, this side chain was placed at C-5. One of the methyl groups (δ_{H} 2.13, s) was placed at C-1 on the basis of its HMBC correlation with the quaternary carbons at δ_{C} 138.8 (C-1a), 120.2 (C-1), and 153.7 (C-2), and the other methyl group was assigned at C-8 on the basis of the correlations of H₃-14/C-8. The hydroxy groups linked to C-7 and C-2 were confirmed by the chemical shift of the quaternary carbons ($\delta_{\text{C}-7}$ 153.8 and $\delta_{\text{C}-2}$ 153.7). NOESY correlations confirmed the substitution pattern of compound 1. Nuclear Overhauser effects were detected between H-3/H-4, H-4/H-12, H-4/H-13, H₃-OMe/H-12, H₃-13/H-12, H-6/H₃-13, H-9/H₃-14, and H-9/H-10. All of the above evidence confirmed the planar structure of 1 as 2,7-dihydroxy-1,8-dimethyl-5-(1-methoxyethyl)-9,10-dihydrophenanthrene, which has been named jinflexin A.

Jinflexin A (1) showed a zero specific rotation, and the baseline ECD spectrum suggested it to be a racemic mixture, which was also confirmed by the separation of its enantiomers on a Chiralpak IA column using hexane–propan-2-ol (90:10) as eluent. The HPLC-ECD spectra of the separated enantiomers were recorded, which enabled the determination of the absolute configuration by exploiting the solution TDDFT-ECD protocol.^{24,25} In a preliminary Merck Molecular Force Field (MMFF) conformational search of (*S*)-1, 31 conformers were generated, which were then reoptimized at both the B3LYP/6-31G(d) in vacuo and B97D/TZVP^{26,27} PCM/CHCl₃ levels, resulting in five and six low-energy conformers above a 2% Boltzmann population, respectively. Jinflexin A (1) has an inherently chiral substituted biphenyl chromophore, of which the conformational freedom is restricted by an ethylidene linker. Similar to atropisomeric biphenyls, the populations of the preferred *P*- or *M*-helicity conformers determine the features of the ECD spectra, which, in turn, are governed by the absolute configuration of the benzylic chirality center. According to literature data of substituted 9,10-dihydrophenanthrene derivatives with an *ortho*-tetrasubstituted biphenyl moiety,^{28,29} *P*- and *M*-helicity conformers can be interconverted at ambient temperature by flipping the C-9 and C-10. The conformational analysis identified conformers with both *P*- and *M*-helicity of the biphenyl moiety, which showed near mirror-image computed ECD curves. The lowest energy B3LYP/6-31G(d) in vacuo conformer (conformer A, 63.5%) of (*S*)-1 had *P*-helicity with a 30.78° $\omega_{\text{C}1\text{a},\text{C}4\text{a},\text{C}5\text{a},\text{C}8\text{a}}$ torsional angle (Figure 1), and the C-12–H-12 bond of the benzylic chirality center was near coplanar with the benzene ring ($\omega_{12\text{H},\text{C}12,\text{C}5,\text{C}5\text{a}} = 12.18^\circ$). The computed

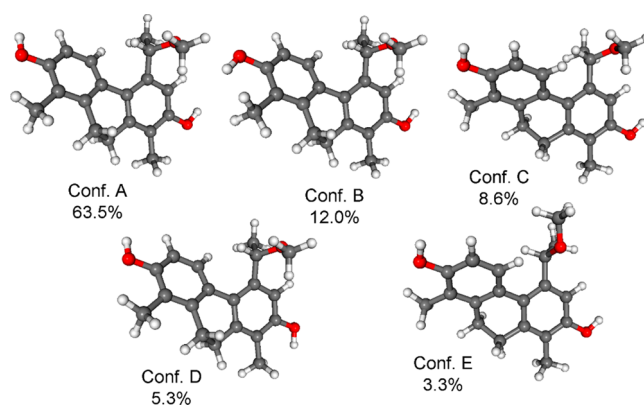


Figure 1. Structures and populations of the low-energy B3LYP/6-31G(d) in vacuo conformers ($\geq 2\%$) of (*S*)-1.

ECD spectra of this conformer reproduced well the experimental HPLC-ECD curve of the first-eluting enantiomer, and conformers B (12.0%) and D (5.3%), differing only in the orientation of the OH-2 and OH-5 protons, showed near congruent computed ECDs. In contrast, conformers C (8.6%) and E (3.3%), having *M*-helicity with -32.78° and -31.20° $\omega_{\text{C}1\text{a},\text{C}4\text{a},\text{C}5\text{a},\text{C}8\text{a}}$ torsional angles, respectively, showed mirror-image computed ECD curves of the experimental ECD (Figure 2, Table 2). Thus, the proper estimation of the population for

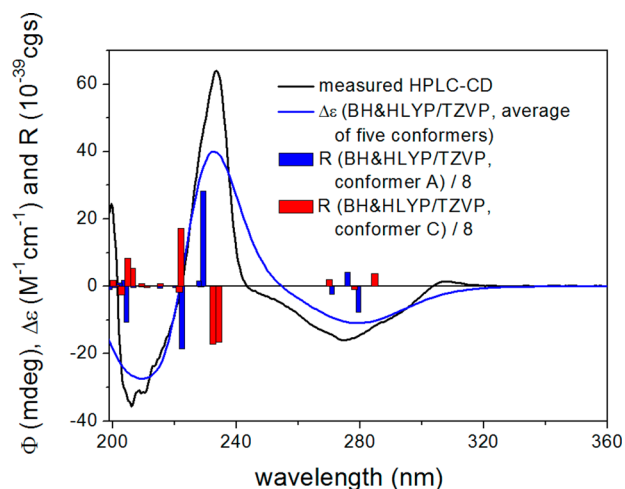


Figure 2. Experimental HPLC-ECD spectrum of the first-eluting enantiomer of 1 in hexane–propan-2-ol (9:1) compared with the Boltzmann-weighted BH&HLYP/TZVP ECD spectrum of (*S*)-1 computed for the B3LYP/6-31G(d) in vacuo conformers. Bars represent the rotational strength of conformers A and C.

the *P*- and *M*-helicity conformers is fundamental for the unambiguous assignment of the absolute configuration.³⁰ It was

Table 2. Selected Geometrical Parameters of the Computed B3LYP/6-31G(d) in Vacuo Conformers of (*S*)-1

	helicity of biphenyl	$\omega_{\text{C}1\text{a},\text{C}4\text{a},\text{C}5\text{a},\text{C}8\text{a}}$	$\omega_{12\text{H},\text{C}12,\text{C}5,\text{C}5\text{a}}$	distance of 4-H and 13-H (Å)
conformer A	<i>P</i>	30.78°	12.18°	2.13
conformer B	<i>P</i>	31.48°	11.85°	2.13
conformer C	<i>M</i>	-32.78°	27.27°	4.18
conformer D	<i>P</i>	31.69°	11.22°	2.13
conformer E	<i>M</i>	-31.20°	-12.86°	4.39

found that the distance of the H-4 and H-13 protons is 2.13 Å in the three *P*-helicity conformers (A, B, and D), while this distance is larger than 4.10 Å for the *M*-helicity conformers (C and E). Since NOE correlation could be observed between H-4 and H-13 protons and there was no correlation between H-4 and H-15, which would be expected from conformers C and E, the *P*-helicity conformers were also confirmed experimentally as the dominant ones in solution. The B97D/TZVP (PCM/CHCl₃) method showed an even smaller contribution of the *M*-helicity forms with a total population of 4.5% from two conformers (Figure S28, Supporting Information). The ECD spectra of (*S*)-**1** computed at the B3LYP/TZVP, BH&HLYP/TZVP, and PBE0/TZVP levels reproduced the experimental HPLC-ECD spectrum of the first-eluting enantiomer, and thus the *S* absolute configuration could be assigned to the enantiomer with a negative Cotton effect (CE) at 275 nm.

Compound **2** was obtained as an amorphous solid; it gave a molecular formula of C₁₉H₂₀O₃ as determined by HRESIMS, through the presence of a peak at *m/z* 297.1392 [M + H]⁺ (calcd for C₁₉H₂₁O₃, 297.1380). The ¹H and ¹³C NMR spectra suggested a 9,10-dihydrophenanthrene skeleton with vinyl substitution, similar to that of juncusol (**7**),³¹ isolated previously from other *Juncus* species (*J. acutus*, *J. effusus*, and *J. roemerianus*) (Table 1).¹³ The differences found were that a hydroxymethyl group instead of the methyl group is linked to the skeleton at position C-1, and a methoxy group (δ_H 3.84, δ_C 56.1) could be placed at C-2 according to its HMBC correlation with C-2 (δ_C 157.4). The position of the hydroxymethyl group was determined by the HMBC cross-peaks between methylene protons (H-11) and C-1, C-1a, and C-2. Nuclear Overhauser effects were observed between OMe-2/H-3, H-3/H-4, H-12/H-14, H-13/H-14, H-8/H-9, and H-10/H₂-11. All this evidence confirmed the structure of **2** (jinflexin B) as 7-hydroxy-6-methyl-1-hydroxymethyl-2-methoxy-5-vinyl-9,10-dihydrophenanthrene.

Compound **3** was isolated as an amorphous, yellow powder, with [α]_D²⁶ −19 (*c* 0.2, MeOH). Its HRESIMS provided a molecular formula of C₁₈H₂₀O₃ through the presence of a peak at *m/z* 285.1498 [M + H]⁺ (calcd for C₁₈H₂₁O₃, 285.1485). The ¹H and ¹³C NMR chemical shifts at δ_H 2.24, 2.65, 2.57, and 2.84 and δ_C 21.1 and 25.1 (C-9, C-10) confirmed a dihydrophenanthrene structure of **3**. The ¹H NMR spectrum exhibited two methyl singlets at δ_H 1.32 and 2.15, two *ortho*-coupled aromatic protons at δ_H 7.23 (*J* = 8.6 Hz) and 6.71 (*J* = 8.5 Hz), and a vinylic system at δ_H 5.13, 4.90, and 6.10 (C-12, C-13) (Table 3). The ¹H–¹H-COSY correlations of the protons at δ_H 2.72, 2.98, and 3.88 and the chemical shifts of their carbons (δ_C 33.6 and 74.4) indicated a –CH₂–CH(OH)– unit (–C-5–C-6–) in the molecule. This structural part was found to form a keto-substituted six-membered ring together with quaternary carbons at δ_C 149.4, 128.8, and 55.5, according to the long-range correlations between H-5 and C-7, C-4a, C-8a, C-5a; H-6 and C-12, C-14; and H-12/C-8, as shown in structural formula **3**. The methyl and vinyl substitution at C-7 was indicated by the HMBC cross-peaks between H₂-13/C-12 and C-7 as well as H₃-14 and C-6, C-7, C-8, and C-12, respectively. In the HSQC spectrum, the protons of the methyl group at δ_H 2.15 (H-11) were correlated to the carbon at δ_C 11.4 (C-11) and had HMBC correlations with C-1, C-1a, and C-2. There was a hydroxy group present at position C-2, which was suggested by the HMBC correlations between C-2 (δ_C 159.4)/H-3 and H-4. All the above evidence obtained confirmed the planar structure of **3** (jinflexin C). The

Table 3. NMR Spectroscopic Data (400 MHz, CD₃OD) for Jinflexin C (**3**)

position	δ _H (<i>J</i> in Hz)	δ _C , type
1		123.1, C
1a		140.1, C
2		159.4, C
3	6.71, d (8.4)	113.6, CH
4	7.23, d (8.4)	125.2, CH
4a		126.4, C
5	2.98, m; 2.72, m	33.6, CH ₂
5a		149.4, C
6	3.88, dd (9.6, 4.5)	74.4, CH
7		55.5, C
8		201.9, C
8a		128.8, C
9	2.65, m; 2.24, m	21.1, CH ₂
10	2.84, m; 2.57, m	25.1, CH ₂
11	2.15, s	11.4, CH ₃
12	6.10, dd (17.7, 10.8)	138.1, CH
13	5.13, d (10.8), 4.90, d (17.7)	116.5, CH ₂
14	1.32, s	20.2, CH ₃

(6*S**,7*S**) relative configuration of **3** was determined on the basis of NOE correlations observed between *α*-oriented H-5 (δ_H 2.98, m) and H-6 and the *β*-oriented H-5 (δ_H 2.72 m) and H-12.

In contrast to **1**, **3** was found to be optically active with a negative specific rotation, and a distinct ECD spectrum could be recorded as well. In order to check on the possibility of partial racemization, chiral HPLC analysis of **3** was carried out under the same conditions used for **1** (Chiralpack IA, hexane–propan-2-ol, 90:10), which showed an 80% enantiomeric excess. HPLC-ECD measurements and HPLC-ECD traces confirmed the enantiomeric relationship of the separated components. For the determination of the absolute configuration, the same ECD calculation protocol was carried out as for **1**. The initial MMFF conformational search of the arbitrarily chosen (6*S*,7*S*) enantiomer yielded 96 conformers, which were reoptimized at the B3LYP/6-31G(d) level in vacuo (Figure S32, Supporting Information) and the B97D/TZVP PCM/CH₃CN level, resulting in 10 and 12 conformers above 2%, respectively. In the lowest energy B3LYP/6-31G(d) conformer, the C-7 vinyl group adopted an axial orientation, while OH-6 has an equatorial orientation. This conformation of ring C was represented by seven other computed conformers totaling 71.1% of the population, and an equatorial C-7 vinyl group was found in conformers C and J with a total population of 10.1%. The structures of the low-energy conformers were in agreement with the observed NOE correlations of **3**. The ECD spectra of (6*S*,7*S*)-**3** computed for the gas-phase or solvent model conformers gave mirror-image agreement of the experimental ECD recorded in acetonitrile (Figure 3), allowing for the assignment of the absolute configuration for the major enantiomer (second-eluting enantiomer in the chiral HPLC analysis) of **3** as (6*R*,7*R*).

Compound **4** was isolated as an amorphous solid, with [α]_D²⁶ 0 (*c* 0.1, MeOH). The HRESIMS (*m/z* 513.2448 [M + H]⁺) established a molecular formula of C₃₆H₃₂O₃ (calcd for C₃₆H₃₃O₃, 513.2424), suggesting the dimeric nature of compound **4**. In the JMOD spectrum, the presence of 36 signals was detected (Table 4). The ¹H NMR spectrum showed sharp singlets for the H-11, H-11', H-14, and H-14' methyls,

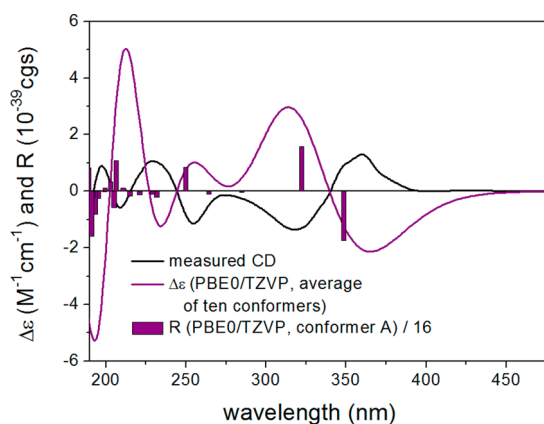


Figure 3. Experimental ECD spectrum of **3** in CH_3CN compared with the Boltzmann-weighted PBE0/TZVP ECD spectrum of (6*S*,7*S*)-**3** computed for the B3LYP/6-31G(d) in vacuo conformers. Bars represent the rotational strength of the lowest energy conformer.

Table 4. NMR Spectroscopic Data (500 MHz, $\text{DMSO}-d_6$) for Jinflexin D (**4**)

position	δ_{H} (J in Hz)	δ_{C} , type	HMBC (H→C)
1		117.1, C	
1a		131.6, C	
2		152.9, C	
3	7.02, d (8.9)	116.4, CH	1, 2, 4a
4	7.59, d (9.0)	119.9, CH	1a, 2, 5a
4a		122.7, C	
5	7.69, s	120.3, CH	4a, 7, 12
5a		128.0, C	
6		141.6, C	
7		133.2, C	
8	7.67, s	128.8, CH	5a, 6, 9, 14
8a		128.1, C	
9	7.64, d (9.2)	126.1, CH	1a, 5a
10	7.74, d (9.2)	121.7, CH	1, 1a, 4a
11	2.41, s	10.9, CH_3	1, 1a, 2
12	4.90, d (8.6)	32.0, CH	5, 5', 6, 6', 7, 7', 13, 13'
13	2.85, m; 2.40, m	28.7, CH_2	6, 6', 12, 12', 13'
14	2.68, s	19.3, CH_3	6, 7, 8
1'		120.3, C	
1a'		138.5, C	
2'		153.9, C	
3'	6.77, d (8.3)	111.6, CH	1', 2', 4a'
4'	7.13, d (8.3)	127.1, CH	1a', 2', 5a'
4a'		125.4, C	
5'		128.4, C	
5a'		125.7, C	
6'		124.5, C	
7'		149.8, C	
8'		121.4, C	
8a'		136.5, C	
9'	2.91, dt (4.3) 2.36, m	26.1, CH_2	1a', 5a', 8', 8a', 10'
10'	2.98, dt (4.1) 2.50, m	25.3, CH_2	1', 1a', 4a', 8a', 9'
11'	2.26, s	11.7, CH_3	1', 1a', 2'
12'	6.96, dd (9.7, 2.7)	128.0, CH	6', 13
13'	5.71, ddd (9.7, 7.1, 2.1)	122.8, CH	5', 12, 13
14'	2.09, s	12.6, CH_3	7', 8', 8a'

doublets for H-3, H-4, H-9, H-10, H-3', and H-4', aromatic singlets for the H-5 and H-8 protons, and signals for H-12' and H-13' (Table 4). According to the NMR data, one of the monomers is a tetrasubstituted phenanthrene containing two methyls and one hydroxy group and a trisubstituted carbon, while the other part of the molecule is a dihydrophenanthrene substituted with two methyls and two hydroxy groups. The linkage between these units was determined on the basis of ^1H , ^1H -COSY and HMBC experiments (Figure 4). The ^1H , ^1H -

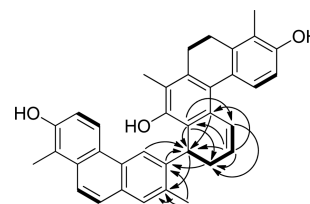


Figure 4. Diagnostic COSY (bold lines) and HMBC correlations (→) for **4**.

COSY spectrum defined the structural fragment $-\text{CHCH}_2-\text{CH}=\text{CH}-$ with the relevant correlated protons (H-12–H-13–H-13'–H-12'). The H-12 proton was correlated in the HMBC spectrum with C-5, C-5', C-6, C-6', C-7, C-7', and C-13'. The long-range correlations of the H-13 protons with the C-6, C-6', HC-12, C-12', and C-13' carbons also indicated linkages to occur between C-12/C-6' and C-13/C-13' of the units, forming a new ring system containing a tri- and a tetracyclic unit. Most probably, during the biosynthesis process, two vinyl-substituted phenanthrene monomers were connected through their vinyl groups, producing a new ring. The HMBC spectroscopic long-range correlations observed between H₃-11/C-1, C-1a, and C-2; H₃-14/C-8, C-8a, and C-7; H₃-11'/C-1', C-1a', and C-2'; and H₃-14'/C-8', C-8a', and C-7' indicated the C-1, C-7, C-1', and C-7' positions of methyl groups and the C-2, C-2', and C-7' positions of hydroxy groups, respectively. The NOESY correlations between H-3/H-4, H-4/H-5, H-8/H-3-14, H-9/H-10, H-10/H-11, H-13-14/H-12 and H-13, H-13/H-13', H-12'/H-13', H-4'/H-12', H-11'/H-10', H-9'/H-14' confirmed the proposed structure of the molecule. On the basis of the above findings, the structure of this compound (jinflexin D) was established as depicted in structural formula **4**.

Although a distinct ECD spectrum for **4** could be recorded in acetonitrile, chiral HPLC analysis showed only 9% enantiomeric excess, and the HPLC-ECD spectra of the separated enantiomers were also recorded. DFT reoptimization of the initial 40 MMFF conformers generated for the arbitrarily chosen (*R*)-**4** yielded nine and nine low-energy conformers ($\geq 2\%$) at B3LYP/6-31G(d) in vacuo and B97D/TZVP PCM/ CHCl_3 levels, respectively. The B97D/TZVP PCM/ CHCl_3 conformers differed only in the orientation of the OH protons, while the relative arrangement of the fused tricyclic and tetracyclic units was near identical (Figure S36, Supporting Information). The ECD spectra of (*R*)-**4** computed for the B97D/TZVP PCM/ CHCl_3 conformers and the Boltzmann-weighted ECD curve reproduced well the HPLC-ECD spectrum of the second-eluting enantiomer of **4** (Figure 5), and it was a mirror image of the experimental solution ECD spectrum. Thus, the absolute configuration of the first-eluting enantiomer of **4** was determined unambiguously as *R*, with the

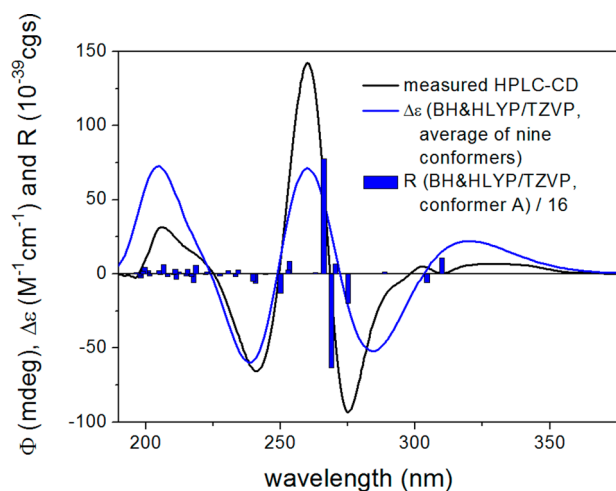


Figure 5. Experimental HPLC-ECD spectrum (first-eluting enantiomer) of **4** in hexane–propan-2-ol (9:1) compared with the Boltzmann-weighted BH&HLYP/TZVP PCM/CHCl₃ ECD spectrum of (*R*)-**4** computed for the B97D/TZVP PCM/CHCl₃ conformers. Bars represent the rotational strength of the lowest energy conformer.

enantiomeric excess derived from the *S* enantiomer (second-eluting enantiomer).

Compound **4** may be considered as being derived by the coupling of 2-hydroxy-1,7-dimethyl-6-vinylphenanthrene (dehydrojuncuenin A, **9**) with 2,7-dihydroxy-1,8-dimethyl-5-vinyl-9,10-dihydrophenanthrene through their vinyl groups, forming an unprecedented heptacyclic structure. Previously, phenanthrene dimers were published from *J. acutus* and *J. effusus*, but in those compounds either no or only one vinyl group was found to be involved in the dimerization.^{15–18}

Besides the new compounds (**1–4**), four dihydrophenanthrenes [juncuenin A (**5**), juncuenin B (**6**), juncusol (**7**), juncuenin D (**8**)], three phenanthrenes [dehydrojuncuenin A (**9**), dehydrojuncusol (**10**), dehydrojuncuenin B (**11**)], and the flavonoid chrysoeriol were isolated from the roots of *J. inflexus*. Their structures were determined by analysis of their MS and 1D and 2D NMR data and by comparison with literature values.^{32–35} In the case of juncuenin B (**6**), juncusol (**7**), juncuenin D (**8**), dehydrojuncusol (**10**), and dehydrojuncuenin B (**11**) the previously published NMR data were completed with ¹H and ¹³C NMR data determined in methanol or dimethyl sulfoxide (see Supporting Information).

Although juncuenin D (**8**) is a chiral derivative, it had been isolated previously as a racemic mixture, and thus characterization of its enantiomers was not reported.³² The present chiral HPLC analysis of **8** showed 4% enantiomeric excess, which was not sufficient to record an acceptable solution ECD spectrum. Thus, the HPLC-ECD spectra of the separated enantiomers were recorded and ECD calculations were performed to assign the absolute configuration. The 13 initial MMFF conformers of the arbitrarily chosen (*S*)-**8** were reoptimized at B3LYP/6-31G(d) in vacuo and B97D/TZVP PCM/CHCl₃ levels, resulting in six and nine low-energy conformers above 2%, respectively. Two groups of the low-energy B3LYP/6-31G(d) in vacuo conformers (Figure 6) could be distinguished based on the relative orientation of the vinyl group. Conformers of the two groups had substantially different computed ECD curves, as represented by conformers A and B. The Boltzmann-weighted ECD spectra of the B3LYP/6-31G(d) in vacuo conformers of (*S*)-**8** (Figure 7) reproduced

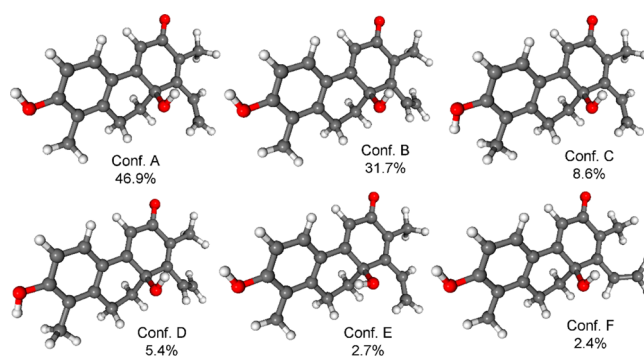


Figure 6. Structures and populations of the low-energy B3LYP/6-31G(d) in vacuo conformers ($\geq 2\%$) of (*S*)-**8**.

well the HPLC-ECD spectrum of the second-eluting enantiomer of **8**, allowing the determination of absolute configuration for the separated enantiomers.

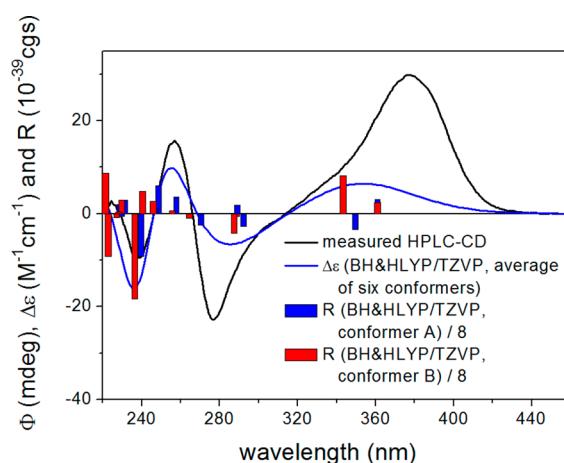


Figure 7. Experimental HPLC-ECD spectrum of the second-eluting enantiomer of **8** in hexane–propan-2-ol (9:1) compared with the Boltzmann-weighted BH&HLYP/TZVP ECD spectrum of (*S*)-**8** computed for the B3LYP/6-31G(d) in vacuo conformers. Bars represent the rotational strength of conformers A and B.

All compounds obtained in the present investigation were isolated for the first time from *J. inflexus*. The methyl group at C-1, a hydroxy group at C-2, and the vinyl, methyl, and hydroxy group substitution on ring B are characteristic features of the isolated phenanthrenes. In compounds **3** and **8**, a carbonyl group can be found in each molecule. In the case of *J. inflexus*, the main compound is juncuenin B (**6**), occurring at up to 0.024% w/w at the roots. For the new compounds (**1**, **3**, **4**) and **8** the absolute configuration was determined by HPLC-ECD measurements and TDDFT-ECD calculations.

The wetland *Juncus* plants (e.g., *J. acutus*, *J. roemerianus*, and *J. effusus*) are considered rich sources of nitrogen-free alkylated phenanthrenoids; the first example of this class was juncusol (**7**) isolated from *J. roemerianus*.³⁶ To date, more than 90 phenanthrenes were isolated from five *Juncus* species (*J. acutus*, *J. effusus*, *J. roemerianus*, *J. setchuensis*, and *J. subulatus*).^{13,37,38} Among them, *J. acutus* and *J. effusus* are the most abundant sources of phenanthrenes.

The *n*-hexane, dichloromethane, and ethyl acetate fractions of a methanol extract prepared from the roots of the plant were evaluated for their antimicrobial effects against methicillin-

resistant *Staphylococcus aureus*, extended-spectrum β -lactamase (ESBL)-producing *Citrobacter freundii*, *Escherichia coli*, *Enterobacter cloacae*, *Klebsiella pneumoniae*, multidrug-resistant *Acinetobacter baumannii*, and *Pseudomonas aeruginosa*. The dichloromethane fraction possessed high antibacterial activity (diameter of inhibition zone: 14.6 ± 1.2 mm) against only methicillin-resistant *Staphylococcus aureus*, while *n*-hexane and ethyl acetate fractions proved to be inactive. The compounds isolated from this fraction were tested for their anti-MRSA activity (Table 5). Among the isolated phenanthrenes, noteworthy inhibitory activities were recorded for jinflexin B (2), juncusol (7), juncuenin D (8), and dehydrojuncuenin B (11). Juncuenin D (8, inhibition zone 12.0 ± 0.3 mm, MIC $12.5 \mu\text{g/mL}$) and juncusol (7, inhibition zone 12.0 ± 0.6 mm, MIC $25 \mu\text{g/mL}$) were the most potent in inhibition of MRSA (ATCC43300) growth, in accordance with previously reported studies.^{5,6} Moreover, dehydrojuncuenin B (11, inhibition zone 10.0 ± 0.2 mm, MIC $25 \mu\text{g/mL}$) and jinflexin B (2, inhibition zone 7.0 ± 0.1 mm, MIC $100 \mu\text{g/mL}$) possessed marked activity. The other compounds proved to be inactive against MRSA. In a previous study, the antibacterial activity of dehydroeffusol and juncusol (7) isolated from *J. effusus* was tested against methicillin-resistant and -sensitive *S. aureus*. It was observed that the activity of the compounds increased 16- and 2-fold, respectively, by irradiation with UVA.³⁹

Table 5. Anti-MRSA Activity of Isolated Compounds

compound	MRSA (ATCC43300) inhibitory activity	
	inhibition (diameter of inhibition zone in mm)	MIC ($\mu\text{g/mL}$)
1	inactive	
2	7.0 ± 0.1	100
3	inactive	
4	inactive	
5	inactive	
6	inactive	
7	12.0 ± 0.6	25
8	12.0 ± 0.3	12.5
9	inactive	
10	inactive	
11	10.0 ± 0.2	25
chrysoeriol	inactive	
vancomycin ^a	15.5 ± 0.6	2

^aPositive control: vancomycin (5 $\mu\text{g/disk}$).

EXPERIMENTAL SECTION

General Experimental Procedures. Vacuum liquid chromatography (VLC) was carried out on silica gel G (15 μm , Merck), and LiChroprep RP-18 (40–63 μm , Merck) was used for reversed-phase VLC. Column chromatography (CC) was performed on polyamide (MP Biomedicals) and Sephadex LH-20 (25–100 μm , Pharmacia Fine Chemicals); preparative thin-layer chromatography (preparative TLC), on silica gel 60 F₂₅₄ plates (Merck). Medium-pressure liquid chromatography (MPLC) was performed by a Biotage SP1 purification system using a KP-C18HS 40+M column. HPLC analyses were performed with a Shimadzu LC-10AT pump interface equipped with a Shimadzu SPD-20A UV–vis detector using a Luna phenyl-hexyl column.

ECD spectra were recorded on a JASCO J-810 spectropolarimeter. NMR spectra were recorded in CD₃OD and DMSO-*d*₆ on a JEOL ECS 400 MHz FT-NMR spectrometer at 400 MHz (¹H) and 100 MHz (¹³C), with tetramethylsilane as internal standard, and on a

Bruker Avance DRX 500 NMR spectrometer at 500 MHz (¹H) and 125 MHz (¹³C). The signals of the deuterated solvents were taken as reference. Two-dimensional (2D) experiments were performed with standard JEOL or standard Bruker software. In the COSY, HSQC, and HMBC experiments, gradient-enhanced versions were applied. Two-dimensional data were acquired and processed with standard JEOL software. High-resolution MS data were recorded on a Waters-Micromass Q-TOF Premier mass spectrometer equipped with an electrospray source. The resolution was over 1 ppm. The data were acquired and processed with MassLynx software.

HPLC-ECD analysis: Chiral HPLC separations were performed with a JASCO HPLC system using a Chiralpak IA column with 250 mm \times 4.6 mm i.d., 5 μm (Daicel, Chemical Industries, Ltd.), and *n*-hexane–propan-2-ol as eluent at a flow rate of 1.0 mL/min. HPLC-UV and OR chromatograms were recorded with a JASCO MD-910 multiwavelength and OR-2090Plus chiral detector, respectively. The online ECD and UV spectra were measured simultaneously by stopping the flow at the UV absorption maximum of each peak. The values of the ECD ellipticity (ϕ) were not corrected for the concentration. Three consecutive scans were recorded and averaged for an HPLC-ECD spectrum with standard sensitivity, 2 nm bandwidth, and 1 s response. The background HPLC-ECD spectrum of the eluent was recorded in the same way.

Plant Material. The roots and aerial parts of *J. inflexus* were collected in June 2014 from the Southern Great Plain (46°24'14.42" N 20°20'53.08" E), Hungary, and identified by Gusztáv Jakab (Institute of Environmental Sciences, Szent István University, Szarvas, Hungary). A voucher specimen (No. 863) has been deposited at the Department of Pharmacognosy, University of Szeged.

Extraction and Isolation. The air-dried and powdered roots of *J. inflexus* (3.5 kg) were extracted with MeOH (60 L) at room temperature in a percolator. The crude extract was evaporated under reduced pressure (393 g) and subjected to solvent–solvent partitioning first with 3.5 L of *n*-hexane, then with 5 L of CH₂Cl₂, and finally with EtOAc (5 L). After concentration, the CH₂Cl₂ fraction (52.81 g) was chromatographed on a polyamide column (150 mm \times 350 mm) with mixtures of MeOH and H₂O [2:3, 1:1, 3:2, 4:1, 1:0 (2.5, 5, 10, 40, and 5 L, respectively); each eluent was collected as a fraction]. The fractions were concentrated and monitored by thin-layer chromatography using cyclohexane–EtOAc–EtOH (20:10:1) as the solvent system. According to their TLC chromatograms, the fractions obtained from the polyamide column with methanol–water (3:2 and 4:1) were similar, so these fractions were combined (J3). The four fractions (J1–4) obtained from the polyamide column were subjected to antibacterial screening, and, among them, J3 showed the most potent inhibitory activity against two MRSA strains (ATCC43300, -64326) (inhibition zones = 15.3 ± 0.6 and 14.3 ± 0.6 mm, respectively), while J2 (inhibition zones = 7.3 ± 0.6 mm for both strains) and J4 (inhibition zones = 7.6 ± 0.6 mm for both strains) possessed moderate activity, and J1 proved to be inactive. Fraction J3 (32.9 g) was further chromatographed by VLC (Kieselgel GF₂₅₄, Merck) on silica gel with a gradient system of cyclohexane–EtOAc–EtOH [from 95:5:0 to 5:5:1 (1000 mL/eluent) and finally with EtOH (1500 mL); volume of collected fractions 100 mL] to yield the major fractions (J3/1–14) according to their TLC patterns (detection at 254 and 366 nm and at daylight after staining with vanillin–sulfuric acid reagent and heating at 120 °C for 5 min).

From fraction J3/3 (35.9 mg), compound 5 (16.2 mg) was crystallized (from methanol). Fraction J3/4 (71.8 mg) was purified on a Sephadex LH 20 column using MeOH as eluent (120 mL; volume of collected fractions 3 mL) to afford compound 9 (21.6 mg). Compounds 10 (35.5 mg) and 7 (12.2 mg) were purified from fraction J3/6 (93.7 mg) by preparative TLC on silica gel 60 F₂₅₄ plates using cyclohexane–EtOAc (7:3) as solvent system.

Fraction J3/7 (3.6 g) was separated by VLC, by elution with a gradient system of *n*-hexane–CH₂Cl₂–MeOH [from 3:7:0 to 0:97:3 (500 mL/eluent) and finally MeOH (500 mL); volume of collected fractions 100 mL] to yield six subfractions. Subfraction J3/7/3 (668 mg) was separated by VLC using a gradient solvent system of CHCl₃–acetone [from 99:1 to 4:1 (200 mL/eluent) and finally acetone (200

mL); volume of collected fractions 20 mL] to yield six subfractions. Furthermore, subfraction J3/7/3/3 (84 mg) was purified by reversed-phase VLC using a MeOH–H₂O gradient elution procedure [from 3:2 to 85:15 (150 mL/eluent) and finally MeOH (150 mL); volume of the collected fractions 12 mL] to yield six subfractions. Subfraction J3/7/3/3/4 (12 mg) was purified on a Sephadex LH-20 column, using MeOH–CH₂Cl₂ (1:1) as eluent (90 mL; volume of collected fractions 2 mL), to afford compound 4 (4.1 mg). Furthermore, from J3/7/4 (1.1 g) and J3/7/6 (1.5 g) compound 6 was crystallized (from methanol, 849 mg). Subfraction J3/7/5 (324 mg) was separated on a Sephadex LH-20 column, using MeOH as eluent (80 mL; volume of collected fractions 2 mL) to afford compound 1 (52.1 mg).

Fraction J3/11 (370 mg) was subjected to RP-MPLC on a Biotage SNAP KP-C18HS 40+M column using a gradient system of MeOH–H₂O [from 1:1, 3:2, 4:1 and finally with MeOH (300 mL each), at a flow rate of 6 mL/min; volume of collected fractions 9 mL] to yield 12 subfractions. Compound 3 (7.5 mg) was obtained from fraction J3/11/4 (11.0 mg) using preparative TLC on silica gel 60 F₂₅₄ plates with CH₂Cl₂–MeOH (95:5) as solvent system. Subfraction J3/11/8 (23.3 mg) was chromatographed on a Sephadex LH-20 column using the mobile phase MeOH (100 mL; volume of collected fractions 3 mL) to afford compounds 2 (6.7 mg) and 8. Final purification of compound 8 (5.2 mg) was performed by RP-HPLC on a Shimadzu LC-10AT instrument with an SPD-20A UV–vis detector using a Luna phenyl-hexyl column (250 × 10 mm, 5 μm), eluted with MeOH–H₂O (7:3) at 2 mL/min (*t_R* 21.5 min). Subfraction J3/11/10 (25.2 mg) was further chromatographed on a Sephadex LH-20 column using the mobile phase MeOH (200 mL; volume of collected fractions 4 mL) to obtain compound 11 (3.8 mg).

Fraction J3/12 (405 mg) was further separated by reversed-phase VLC with a gradient system of MeOH–H₂O [from 3:7 to 9:1 (100 mL/eluent) and finally MeOH (200 mL); volume of collected fractions 15 mL] to yield 10 subfractions. From subfraction 4, chrysoeriol (6.1 mg) was isolated by the use of preparative TLC, using CH₂Cl₂–MeOH (95:5) as solvent system.

(±)-*Jinflexin A (1)*: amorphous solid; [α]_D²⁶ 0 (*c* 0.1, MeOH); UV (CH₃CN) λ_{\max} (log ϵ) 276 (4.01), 211 (4.50) nm; ¹H and ¹³C NMR data, see Table 1; (+)-HRESIMS *m/z* 321.1532 [M + Na]⁺ (calcd for C₁₉H₂₂O₃Na, 321.1461).

(S)-**1**: *t_R* 5.51 min on a Chiralpak IA column (hexane–propan-2-ol, 90:10); HPLC-ECD {hexane–propan-2-ol, 90:10, λ_{\max} (ϕ)} 308 (1.51), 292sh (–8.37), 275 (–15.91), 233.5 (63.95), 210 (–31.40) nm; (R)-**1**: *t_R* 5.93 min on a Chiralpak IA column (hexane–propan-2-ol, 90:10); HPLC-ECD {hexane–propan-2-ol, 90:10, λ_{\max} (ϕ)} 308 (–1.32), 292sh (6.80), 275 (13.72), 233.5 (–52.72), 210 (19.89) nm.

Jinflexin B (2): amorphous solid; UV (MeOH) λ_{\max} (log ϵ) 280 (3.81), 219 (3.99) nm; ¹H and ¹³C NMR data, see Table 1; (+)-HRESIMS *m/z* 297.1392 [M + H]⁺ (calcd for C₁₉H₂₁O₃⁺, 297.1380).

Jinflexin C (3): amorphous, yellow powder; [α]_D²⁶ –19 (*c* 0.2, MeOH, 80% ee); UV (CH₃CN) λ_{\max} (log ϵ) 329 (3.75), 242 (3.52), 217sh (3.63), 195sh (4.06) nm; ECD {CH₃CN, λ_{\max} ($\Delta\epsilon$)} 360 (1.36), 351sh (1.02), 319 (–1.35), 255 (–1.22), 228 (1.13), 209 (–0.77) nm; ¹H and ¹³C NMR data, see Table 3; (+)-HRESIMS *m/z* 285.1498 [M + H]⁺ (calcd for C₁₈H₂₀O₃⁺, 285.1485).

(6R,7R)-**3** *t_R* = 15.48 min on a Chiralpak IA column (hexane–propan-2-ol, 90:10); (6S,7S)-**3**: *t_R* = 8.44 on a Chiralpak IA column (hexane–propan-2-ol, 90:10).

Jinflexin D (4): amorphous solid; [α]_D²⁶ 0 (*c* 0.1, MeOH, 9% ee); UV (CH₃CN) λ_{\max} (log ϵ) 361 (3.30), 321sh (3.64), 306sh (4.08), 281sh (4.33), 271sh (4.55), 263 (4.64), 226sh (4.53) nm; ECD {CH₃CN, λ_{\max} ($\Delta\epsilon$)} 331 (–0.12), 301 (–0.24), 288sh (0.10), 275 (1.94), 260 (–2.86), 241 (1.10), 202 (–1.51) nm; ¹H and ¹³C NMR data, see Table 4; (+)-HRESIMS *m/z* 512.2299 [M + H]⁺ (calcd for C₃₆H₃₂O₃⁺, 512.2346).

(R)-**4**: *t_R* 4.38 min on Chiralpak IA column (hexane–propan-2-ol, 80:10); HPLC-ECD {hexane–propan-2-ol, 80:10, λ_{\max} (ϕ)} 331 (6.44), 304 (6.28), 293sh (–6.50), 275 (–103.43), 259 (151.40), 241 (–69.62), 210 (27.05) nm; (S)-**4**: *t_R* 4.77 min on a Chiralpak IA column (hexane–propan-2-ol, 80:10); HPLC-ECD {hexane–propan-

2-ol, 80:10, λ_{\max} (ϕ)} 331 (–7.71), 304 (–7.38), 293sh (6.78), 275 (109.51), 259 (–148.97), 241 (77.25), 210 (–29.04) nm.

Juncuenin B (6): white powder; NMR data were in good agreement with data published for 6 in CDCl₃.³² NMR assignments for CD₃OD solution, made on the basis of 2D measurements, were not published previously (Supporting Information).

Juncusol (7): amorphous solid; ¹H NMR (CD₃OD, 500 MHz) (data measured for the first time in this solvent, Supporting Information).

Juncuenin D (8): yellow powder; UV (CH₃CN) λ_{\max} (log ϵ) 347 (3.88), 275sh (3.85), 251 (4.04), 213 (4.39) nm; ¹H NMR (CD₃OD, 400 MHz) and ¹³C NMR (CD₃OD, 100 MHz) (data measured for the first time in this solvent, Supporting Information).

(R)-**8**: *t_R* 4.72 min on Chiralpak IA column (hexane–propan-2-ol, 80:10); HPLC-ECD {hexane–propan-2-ol, 90:10, λ_{\max} (ϕ)} 376 (–24.82), 275.5 (22.63), 258 (–20.83), 238 (9.32) nm; (S)-**8**: *t_R* 5.20 min on Chiralpak IA column (hexane–propan-2-ol, 80:10); HPLC-ECD {hexane–propan-2-ol, 90:10, λ_{\max} (ϕ)} 376 (29.86), 275.5 (–22.40), 258 (15.23), 238 (–9.46) nm. 4% ee as determined by chiral HPLC.

Dehydrojuncusol (10): amorphous solid; ¹H NMR (DMSO-*d*₆, 400 MHz) and ¹³C NMR (DMSO-*d*₆, 100 MHz) (data measured for the first time in this solvent, Supporting Information).

Dehydrojuncuenin B (11): brown, amorphous powder; ¹H NMR (DMSO-*d*₆, 400 MHz) and ¹³C NMR (DMSO-*d*₆, 100 MHz) (data measured for the first time in this solvent, Supporting Information).

In the case of juncuenin A (**5**) and dehydrojuncuenin A (**9**), the spectroscopic data obtained were identical with those previously published.³²

Test Microorganisms. The test microorganisms were one standard and nine clinical isolates with different antibiotic resistance profiles, which originated from various departments of Albert Szent-Györgyi Health Center and were identified at the Institute of Clinical Microbiology at University of Szeged by conventional methods. The standard strain was methicillin-resistant *Staphylococcus aureus* (ATCC43300). The clinical strains were multiresistant (MR) *Acinetobacter baumannii* (64060/2 and 61748/2), ESBL-positive *Citrobacter freundii* (63458), ESBL-positive *Enterobacter cloacae* (63033), ESBL-positive *Escherichia coli* (64663), ESBL-positive *Klebsiella pneumoniae* (63735), MR *Pseudomonas aeruginosa* (61485/1 and 64658), and methicillin-resistant *S. aureus* (64326). Microbial cultures were grown on standard Mueller-Hinton agar plates and maintained at 4 °C throughout the study to use as stock cultures.

Antibacterial Screening. Antibacterial activities of the fractions and the pure compounds were first screened for their inhibitory zones by a disk-diffusion method. The plant extracts were prepared at 50 mg/mL, while pure compounds were diluted to 10 mg/mL using DMSO. The sterile filter paper disks (6 mm diameter) impregnated with the extracts (50 μL) were placed on the agar plate seeded with the respective bacterial suspension (inoculum 0.5 McFarland, (1–2) × 10⁸ CFU/mL). The solvent served as a negative control. The plates were then incubated at 37 °C for 24 h under aerobic conditions. The diameters of inhibition zones produced by the plant extracts (including the disk) were measured and recorded. All experiments were carried out in triplicate.

The active test compounds with diameters of inhibition zone of ≥10 mm were further investigated to determine their minimal inhibitory concentration (MICs) by a microdilution method. Briefly, in 96-well plates, the stock solutions of the compounds (50 mg/mL in DMSO) were serially diluted with Mueller-Hinton broth to arrive at final concentrations between 2.5 mg/mL and 4.9 μg/mL. Then, 100 μL of inoculum (0.5 McFarland, (1–2) × 10⁸ CFU/mL) was then added to the wells. A sterility check (medium and DMSO in amounts corresponding to the highest concentration), negative control (medium, DMSO, and inoculum), and positive control (medium, DMSO, inoculum, and vancomycin) were included for each experiment. The plates were then incubated at 37 °C for 24 h under an aerobic environment. The MIC of each compound was the lowest concentration that completely inhibited the visible bacterial growth. All experiments were performed twice in triplicate.

Computational Section. Mixed torsional/low-frequency mode conformational searches were carried out by means of the Macro-model 9.9.223 software using the Merck Molecular Force Field with an implicit solvent model for CHCl_3 .⁴⁰ Geometry reoptimizations were carried out at the B3LYP/6-31G(d) level in vacuo and the B97D/TZVP level^{26,27} with the PCM solvent model for CH_3CN or CHCl_3 . TDDFT ECD calculations were run with various functionals (B3LYP, BH&HLYP, PBE0) and the TZVP basis set as implemented in the Gaussian 09 package with the same or no solvent model as in the preceding DFT optimization step.⁴¹ ECD spectra were generated as sums of Gaussians with 3000 cm^{-1} widths at half-height (corresponding to ca. 24 at 280 nm), using dipole-velocity-computed rotational strength values.⁴² Boltzmann distributions were estimated from the ZPVE-corrected B3LYP/6-31G(d) energies in the gas-phase calculations and from the B97D/TZVP energies in the solvated ones. The MOLEKEL software package was used for visualization of the results.⁴³

■ ASSOCIATED CONTENT

📄 Supporting Information

The Supporting Information is available free of charge on the ACS Publications website at DOI: [10.1021/acs.jnatprod.6b00581](https://doi.org/10.1021/acs.jnatprod.6b00581).

ECD spectra of jinflexins A, C, and D and compound **8**; original NMR spectra of jinflexins A–D (**1–4**); ¹H and ¹³C NMR data of compounds **6–8**, **10**, and **11** (PDF)

■ AUTHOR INFORMATION

Corresponding Authors

*Tel (F.-R. Chang): +886-7-3121101 (ext. 2162). Fax: +886-7-3114773. E-mail: aaronfrc@kmu.edu.tw.

*Tel (A. Vasas): +36-62-546451. Fax: +36-62-545704. E-mail: vasasa@pharmacognosy.hu.

Notes

The authors declare no competing financial interest.

■ ACKNOWLEDGMENTS

Financial support from the Hungarian Scientific Research Fund (OTKA K109846) is gratefully acknowledged. A.V. acknowledges the award of a János Bolyai scholarship of the Hungarian Academy of Sciences. T.K. thanks the Hungarian National Research Foundation (OTKA K105871) for financial support and the National Information Infrastructure Development Institute (NIIFI 10038) for CPU time. This work was supported by grants from the Ministry of Science and Technology of Taiwan (NSC 102-2628-B-037-003-MY3, MOST 103-2320-B-037-005-MY2, awarded to F.-R.C.). This study is also supported partially by Kaohsiung Medical University (Aim for the Top Universities Grant, nos. KMU-TP104E39, KMU-TP104A26), Ministry of Health and Welfare of Taiwan (MOHW105-TDU-B-212-134007), and Health and Welfare Surcharge of Tobacco Products. The authors thank G. Jakab (Institute of Environmental Sciences, Szent István University, Szarvas, Hungary) for the identification of the plant and A. Csorba (Department of Pharmacognosy, University of Szeged) for the HRMS measurements.

■ REFERENCES

- (1) Saxena, S.; Gomber, C. *Centr. Eur. J. Med.* **2010**, *5*, 12–29.
- (2) David, M. Z.; Daum, R. S. *Clin. Microbiol. Rev.* **2010**, *23*, 616–687.
- (3) Tsiodras, S.; Gold, H. S.; Sakoulas, G.; Eliopoulos, G. M.; Wennersten, C.; Venkataraman, L.; Moellering, R. C.; Ferraro, M. J. *Lancet* **2001**, *358*, 207–208.
- (4) Gibbons, S. *Phytochem. Rev.* **2005**, *4*, 63–78.
- (5) Hanawa, F.; Okamoto, M.; Towers, G. H. *Photochem. Photobiol.* **2002**, *76*, 51–56.
- (6) Chapatwala, K. D.; de la Cruz, A. A.; Miles, D. H. *Life Sci.* **1981**, *29*, 1997–2001.
- (7) The Plant List. <http://www.theplantlist.org/browse/A/Juncaceae/>.
- (8) Drábková, L.; Kirschner, J.; Seberg, O.; Petersen, G.; Vlcek, C. *Plant Syst. Evol.* **2003**, *240*, 133–147.
- (9) Wang, Y. G.; Wang, Y. L.; Zhai, H. F.; Liao, Y. J.; Zhang, B.; Huang, J. M. *Nat. Prod. Res.* **2012**, *26*, 1234–1239.
- (10) Shima, K.; Toyota, M.; Asakawa, Y. *Phytochemistry* **1991**, *30*, 3149–3151.
- (11) Boulos, L. *Medicinal Plants of North Africa*; Reference Publications, Inc.: Algonac, MI, 1983.
- (12) Harborne, J. B. In *Biosynthesis. The Royal Society of Chemistry, Special Periodical Reports*; Spottiswoode Ballantyne Ltd.: Colchester, UK, 1980; Vol. 6, p 60.
- (13) Kovács, A.; Vasas, A.; Hohmann, J. *Phytochemistry* **2008**, *69*, 1084–1110.
- (14) Della Greca, M.; Fiorentino, A.; Previtera, L.; Zarrelli, A. *Phytochemistry* **1995**, *40*, 533–535.
- (15) Della Greca, M.; Fiorentino, A.; Monaco, P.; Previtera, L.; Temussi, F.; Zarrelli, A. *Tetrahedron* **2003**, *59*, 2317–2324.
- (16) Della Greca, M.; Fiorentino, A.; Monaco, P.; Previtera, L.; Zarrelli, A. *Tetrahedron Lett.* **2002**, *43*, 2573–2575.
- (17) Behery, F. A. A.; Naeem, Z. E. M.; Maatooq, G. T.; Amer, M. M. A.; Ahmed, A. F. *Nat. Prod. Res.* **2013**, *27*, 155–163.
- (18) Ma, W.; Liu, F.; Ding, Y. Y.; Zhang, Y.; Li, N. *Fitoterapia* **2015**, *105*, 83–88.
- (19) Stabursvik, A. *Acta Chem. Scand.* **1968**, *22*, 2056–2057.
- (20) Della Greca, M.; Fiorentino, A.; Monaco, P.; Previtera, L. *Phytochemistry* **1994**, *35*, 1017–1022.
- (21) Della Greca, M.; Fiorentino, A.; Isidori, M.; Previtera, L.; Temussi, F.; Zarrelli, A. *Tetrahedron* **2003**, *59*, 4821–4825.
- (22) Williams, C. A.; Harborne, J. B. *Biochem. Syst. Ecol.* **1975**, *3*, 181–190.
- (23) Yang, G. Z.; Li, H. X.; Song, F. J.; Chen, Y. *Helv. Chim. Acta* **2007**, *90*, 1289–1295.
- (24) Pescitelli, G.; Bruhn, T. *Chirality* **2016**, *28*, 466–474.
- (25) Zhou, Z. F.; Kurtán, T.; Mándi, A.; Geng, M. Y.; Ye, B. P.; Guo, Y. W. *Org. Lett.* **2014**, *16*, 1390–1393.
- (26) Grimme, S. *J. Comput. Chem.* **2006**, *27*, 1787–1799.
- (27) Sun, P.; Xu, D.-X.; Mándi, A.; Kurtán, T.; Li, T.-J.; Schulz, B.; Zhang, W. *J. Org. Chem.* **2013**, *78*, 7030–7047.
- (28) Ohmori, K.; Kitamura, M.; Suzuki, K. *Angew. Chem., Int. Ed.* **1999**, *38*, 1226–1229.
- (29) Bringmann, G.; Price Mortimer, A. J.; Keller, P. A.; Gresser, M. J.; Garner, J.; Breuning, M. *Angew. Chem., Int. Ed.* **2005**, *44*, 5384–5427.
- (30) Mándi, A.; Swamy, M. M. M.; Taniguchi, T.; Anetai, M.; Monde, K. *Chirality* **2016**, *28*, 453–459.
- (31) Miles, D. H.; Bhattacharyya, J.; Mody, N. V.; Atwood, J. L.; Black, S.; Hedin, P. A. *J. Am. Chem. Soc.* **1977**, *99*, 618–620.
- (32) Wang, X.; Ke, C.; Tang, C.; Yuan, D.; Ye, Y. *J. Nat. Prod.* **2009**, *72*, 1209–1212.
- (33) Della Greca, M.; Fiorentino, A.; Mangoni, L.; Monaco, P.; Previtera, L. *Tetrahedron Lett.* **1992**, *33*, 5257–5260.
- (34) Sarkar, H.; Zerezhgi, M.; Bhattacharyya, J. *Phytochemistry* **1988**, *27*, 3006–3008.
- (35) Lee, S.; Han, S.; Kim, H. M.; Lee, J. M.; Mok, S. Y.; Lee, S. J. *Appl. Biol. Chem.* **2011**, *54*, 73–78.
- (36) Miles, D. H.; Bhattacharyya, J.; Mody, N. V.; Atwood, J. L.; Black, S.; Hedin, P. A. *J. Am. Chem. Soc.* **1977**, *99*, 618–620.
- (37) Wang, J.; Liu, J.; Wen, Q.; Li, C.; Li, Y.; Lian, B.; Tang, H.; Yao, T. *Biochem. Syst. Ecol.* **2010**, *38*, 1039–1041.
- (38) Abdel-Razik, A. F.; Elshamy, A.-S. I.; Nassar, M. I.; El-Kousy, S. M.; Hamdy, H. *Rev. Latinoamer. Quím.* **2009**, *37*, 70–84.

(39) Fujinori, H.; Okamoto, M.; Towers, G. H. N. *Photochem. Photobiol.* **2002**, *76*, 51–56.

(40) *MacroModel*; Schrödinger, LLC, 2012, <http://www.schrodinger.com/MacroModel>.

(41) Frisch, M. J.; Trucks, G. W.; Schlegel, H. B.; Scuseria, G. E.; Robb, M. A.; Cheeseman, J. R.; Scalmani, G.; Barone, V.; Mennucci, B.; Petersson, G. A.; Nakatsuji, H.; Caricato, M.; Li, X.; Hratchian, H. P.; Izmaylov, A. F.; Bloino, J.; Zheng, G.; Sonnenberg, J. L.; Hada, M.; Ehara, M.; Toyota, K.; Fukuda, R.; Hasegawa, J.; Ishida, M.; Nakajima, T.; Honda, Y.; Kitao, O.; Nakai, H.; Vreven, T.; Montgomery, J. A., Jr.; Peralta, J. E.; Ogliaro, F.; Bearpark, M.; Heyd, J. J.; Brothers, E.; Kudin, K. N.; Staroverov, V. N.; Kobayashi, R.; Normand, J.; Raghavachari, K.; Rendell, A.; Burant, J. C.; Iyengar, S. S.; Tomasi, J.; Cossi, M.; Rega, N.; Millam, J. M.; Klene, M.; Knox, J. E.; Cross, J. B.; Bakken, V.; Adamo, C.; Jaramillo, J.; Gomperts, R.; Stratmann, R. E.; Yazyev, O.; Austin, A. J.; Cammi, R.; Pomelli, C.; Ochterski, J. W.; Martin, R. L.; Morokuma, K.; Zakrzewski, V. G.; Voth, G. A.; Salvador, P.; Dannenberg, J. J.; Dapprich, S.; Daniels, A. D.; Farkas, O.; Foresman, J. B.; Ortiz, J. V.; Cioslowski, J.; Fox, D. J. *Gaussian 09*, revision B.01; Gaussian, Inc.: Wallingford, CT, 2010.

(42) Stephens, P. J.; Harada, N. *Chirality* **2010**, *22*, 229–233.

(43) Varetto, U. *MOLEKEL*, v. 5.4; Swiss National Supercomputing Centre: Manno, Switzerland, 2009.